

# Morphological Effects on the Physical Properties of Polymer Composites†

Polymer composites have found widespread applications in the past 10 years. Various forms of polymer blends and filled polymers are being used in electronic circuit boards, electrochemical cells, and reinforced structural elements, to name a few. The components are chosen to impart, control, or accentuate selected properties, which may be dielectric, thermal, and electronic properties, chemical selectivity, transport, and stability, or mechanical strength, toughness, and durability. Empirically, the behavior of polymer composites depends critically on details of the dispersion of components, interfacial adhesion, particle size, and, in particular, morphology.<sup>1</sup> Often, divergent behavior from seemingly identical compositions can be traced to morphological differences. Although the transition from an insulator to a conductor or from a brittle composite to a ductile one has been predicted by percolation theory,<sup>2</sup> quantitative computations are usually limited to spherical geometry<sup>2</sup> or idealized conditions that can only be realized on a computer.<sup>3</sup> We present here a simple effective medium formulation<sup>4</sup> that can easily track the influence on physical properties of morphological evolution from lamellar to fibrillar structures. The theory as presented is suitable for both transport and dielectric properties and can be generalized to deal with elastic properties as well.

The starting point of our model is a collection of oriented spheroids<sup>5</sup> of the same material and eccentricity<sup>6</sup>  $e$ . Their axes of revolution are along the direction of applied field. The remaining space is now completely filled with spheroids of a different material but of the same eccentricity and orientation. For simplicity, we shall restrict our discussions below to transport and dielectric properties. The appropriate susceptibilities<sup>7</sup> for the two media are denoted by  $\chi_1$  and  $\chi_2$ , respectively. In the following, only the diagonal component of the  $\chi$  tensor that is along the field direction will be retained because only that component is relevant for the present geometry. A unique feature of this model is that the shape of the inclusions can be continuously altered between lamellar and spherical or between fibrillar and spherical by changing the eccentricity and type of the spheroids.<sup>6</sup> The model is, therefore, useful for both extruded films and spun fibers as either the prolate or the oblate morphology should dominate.

Let us now excise a spheroid composed entirely of the  $i$ th material and immerse it in an effective medium of susceptibility  $\bar{\chi}$  and mean field  $\bar{E}$ . The field inside the spheroid is related to  $\bar{E}$  and  $\bar{\chi}$  by<sup>8</sup>

$$E_i = \bar{E} / \{1 + [(\chi_i / \bar{\chi}) - 1]F(e)\} \quad (1)$$

where

$$F(e) = \frac{1 - e^2}{2e^3} \left\{ \ln \left( \frac{1 + e}{1 - e} \right) - 2e \right\} \quad (2a)$$

for a prolate spheroid and

$$F(e) = \frac{1}{e^2} \left\{ 1 - \left( \frac{(1 - e^2)^{1/2}}{e} \right) \arctan \left( \frac{e}{(1 - e^2)^{1/2}} \right) \right\} \quad (2b)$$

for an oblate spheroid. In the dielectric case,  $F(e)$  is the cavity depolarization factor for the geometry under consideration. Since the effective medium is a statistical average of the two media, the mean field  $\bar{E}$  must, therefore, obey

$$\bar{E} = f_1 E_1 + f_2 E_2 \quad (3)$$

where  $f_i$  is the volume fraction of the  $i$ th medium. Substituting (1) into (3) and using the normalization condition  $f_1 + f_2 = 1$ , we obtain

$$(1 - F(e))\bar{\chi}^2 + \{\chi_1(F(e) - f_1) + \chi_2(F(e) - f_2)\}\bar{\chi} - \chi_1\chi_2F(e) = 0 \quad (4)$$

Equation 4 applies equally well to transport and dielectric phenomena because the dielectric function  $\epsilon(\omega)$  and conductivity  $\sigma(\omega)$  are related:<sup>9</sup>  $\sigma(\omega) = i\omega\epsilon_0\epsilon(\omega)$ , where  $i$  is the imaginary number,  $\omega$  is the frequency, and  $\epsilon_0$  is the free-space permittivity.

Several interesting limits of eq 4 are worth discussing:

(I)  $F(e) = 0$ . This corresponds to perfect striation and represents the most favorable condition for conduction in any composite. The equivalent circuit is resistors or capacitors in parallel. The composite susceptibility  $\bar{\chi}$  is simply a weighted average of the component susceptibilities:

$$\bar{\chi} = f_1\chi_1 + f_2\chi_2 \quad (5)$$

This result is exact and corresponds to the highest upper bound of composite conductivity.

(II)  $F(e) = 1$ . This represents the other one-dimensional (1D) extreme—perfect stratification; the equivalent circuit is now resistors or capacitors in series. The composite susceptibility is therefore

$$\bar{\chi} = \chi_1\chi_2 / (f_2\chi_1 + f_1\chi_2) \quad (6)$$

This result is also exact.

(III)  $F(e) = 1/3$ . This condition corresponds to spherical inclusions and is the dividing line between prolate ( $F < 1/3$ ) and oblate ( $F > 1/3$ ) cases. Equation 4 now reduces to the standard form given in the literature.<sup>4</sup>

(IV)  $\chi_1 = \sigma_1$  and  $\chi_2 = i\omega\epsilon_0\epsilon_2$ . This represents conductive fillers in a dielectric matrix. The effective susceptibility  $\bar{\chi}$  is given by  $(\bar{\sigma} + i\omega\epsilon_0\bar{\epsilon})$ , where  $\bar{\sigma}$  and  $\bar{\epsilon}$  are the effective conductivity and dielectric constant for the composite, respectively. Let us consider the dc limit ( $\omega \rightarrow 0$ ); expanding and keeping terms that are linear in  $\omega$  and solving for the real and imaginary parts of  $\bar{\chi}$ , respectively, we obtain

$$\bar{\sigma} = \sigma_1(1 - F)^{-1}(f_1 - F) \quad \text{for } 1 \geq f_1 \geq F \quad (6a)$$

$$\bar{\sigma} = 0 \quad \text{for } 0 \leq f_1 \leq F \quad (6b)$$

and

$$\bar{\epsilon} = \epsilon_2 f_1(1 - f_1)(1 - F)^{-1}(f_1 - F)^{-1} \quad \text{for } 1 \geq f_1 \geq F \quad (7a)$$

$$\bar{\epsilon} = \epsilon_2 F(F - f_1)^{-1} \quad \text{for } 0 \leq f_1 \leq F \quad (7b)$$

These results indicate an insulator-to-conductor transition at  $f_0 = F$ , the percolation threshold. For oriented spheroids, the dependence of  $f_0$  on morphology is given by eq 2. Equation 6 predicts that the conductivity increases linearly with  $f - f_0$  above the percolation threshold. This is a generalization of the effective medium result normally quoted in the literature to oriented spheroids. In comparison, eq 7 predicts that the dielectric function  $\epsilon$  diverges at the threshold as  $|f_1 - f_0|^{-1}$ . This result<sup>10</sup> has only been obtained previously by using either scaling argument<sup>11</sup> near  $f_0$  or complicated analytical properties<sup>12</sup> of  $\epsilon(\omega)$  and  $\sigma(\omega)$ . It has never been derived by the intuitively more transparent effective medium theory before. The anomalous behavior of  $\epsilon$  is related to the gradual shorting of the composite by the conductive phase. Just below the percolation threshold, extended clusters of conductive spheroids are prevented from connecting into a pervasive conducting network by thin dielectric barriers. These barriers contribute to an enormous capacitance which, upon normalization to the characteristic dimension of the

† Contribution No. 3323.

bulk samples, leads to a huge apparent dielectric constant for the composite medium. Above the threshold, they and their anomalous contributions disappear rapidly because of the formation and expansion of percolation channels.

Although eq 6 and 7 contain all the essential physics of a percolative transition and are quantitatively accurate at either high or low conductor loading, they are often unreliable near the percolation threshold  $f_0$ . Specifically, eq 6 and 7 predict wrong values for the critical exponents<sup>10</sup>  $s$  and  $t$  and too high a threshold  $f_0$ , except for the 1D limits (I) and (II). These turn out to be common features for most mean-field-type theories of phase transitions and stem from the implicit (and often incorrect) assumption that correlation and fluctuation are always negligible. In the present context, the depolarization factor  $F$  of a single spheroid is used for any filler concentration despite widespread clustering near the threshold concentration. This type of correlation can be incorporated into the effective medium theory either perturbatively by the cumulant expansion technique<sup>13</sup> or empirically by using an effective depolarization tensor.<sup>14</sup> To account for critical fluctuations, the effective medium theory has also been phenomenologically augmented with scaling theory.<sup>15</sup> Other approaches that have rigorously included the effects of correlations and fluctuations are numerical simulation,<sup>3</sup> renormalization group theory,<sup>12</sup> and scaling theory.<sup>11</sup> These theories are either too cumbersome to use or unable to model morphological effects conveniently. Finally, critical fluctuations are always small and correlations unimportant for composites in which the two components have sufficiently similar properties,<sup>3</sup> viz.

$$10^{-2} \lesssim \chi_1/\chi_2 \lesssim 10^2 \quad (8)$$

Under such a condition, eq 4 is generally applicable whenever contact resistance and electron tunneling are negligible.

To test this theory, we have applied eq 4 to model the selectivity of  $\text{Na}^+$  and  $\text{OH}^-$  currents in physical blends of two similar but incompatible perfluorinated ionomers.<sup>16</sup> Let CE be the current efficiency of sodium ions:

$$\text{CE} = \sigma_{\text{Na}}/(\sigma_{\text{Na}} + \sigma_{\text{OH}}) \quad (9)$$

where  $\sigma_{\text{Na}}$  and  $\sigma_{\text{OH}}$  are the conductivity of the  $\text{Na}^+$  and  $\text{OH}^-$  ions, respectively. For the ionomers under consideration, the CE of the carboxylate usually exceeds 90% whereas the CE of the sulfonate is well below 70%. Typical pressed films of the blend have a pronounced lamellar morphology as shown in Figure 1. The measured CE is plotted as a function of blend composition and compared to computed CE for oriented oblate spheroids in Figure 2. The theoretical results for three values of the eccentricity (or equivalently the aspect ratio) are shown; other inputs to the calculations are the measured conductivities for the pure ionomers:  $\sigma_{\text{Na}} = 1.8 \times 10^{-2} \Omega^{-1} \text{cm}^{-1}$  and  $\sigma_{\text{OH}} = 1.36 \times 10^{-2} \Omega^{-1} \text{cm}^{-1}$  for the sulfonate phase and  $\sigma_{\text{Na}} = 7 \times 10^{-3} \Omega^{-1} \text{cm}^{-1}$  and  $\sigma_{\text{OH}} = 6 \times 10^{-4} \Omega^{-1} \text{cm}^{-1}$  for the carboxylate phase. The computed CE for the lamellar morphology agrees very well with data. Notice also the dramatic change in CE predicted in Figure 2 as the blend morphology changes from lamellar (top curve) to spherical (bottom curve). Physically, the gradual change in CE predicted for the spherical morphology arises from the ability of hydroxyl ions to shunt the low-conductance carboxylate phase via the surrounding sulfonate phase. As the spheres are deformed into pancakes, the hydroxyl ions are gradually forced to pass through the carboxylate region since the penalty for taking a long tortuous sideways bypass soon exceeds the low conductance inconvenience of going straight ahead. In the ultimate lamellar limit,  $\text{OH}^-$



Figure 1. Cross-sectional micrograph of a pressed film of a 25% carboxylate/75% sulfonate blend of perfluorinated ionomers. The elongated regions (arrows) are the carboxylate phase.

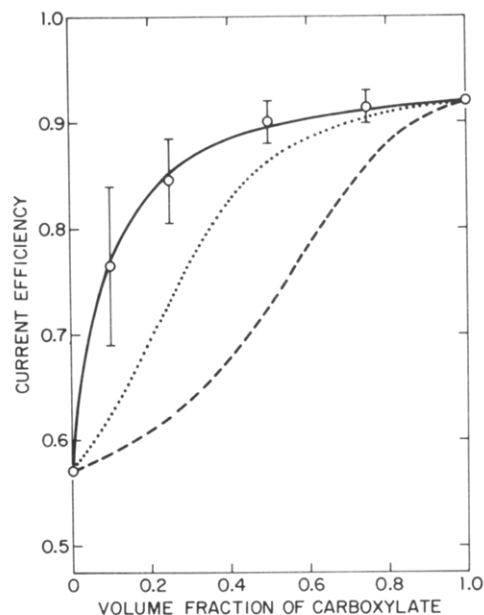
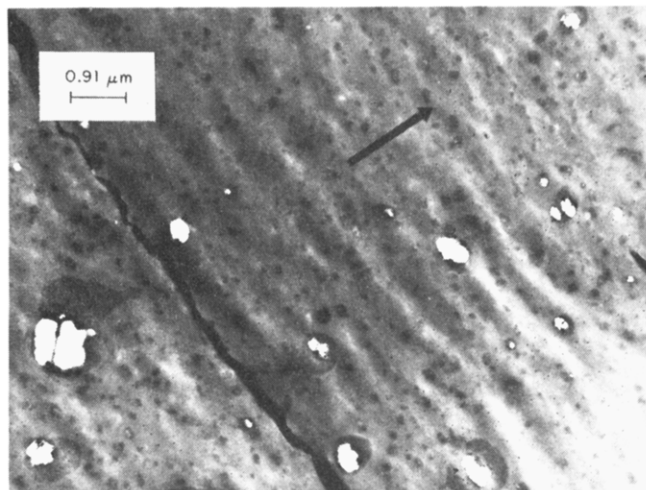


Figure 2. Current efficiency of perfluorinated carboxylate/sulfonate blends. Open circles are average data and vertical bars indicate the range of values actually observed. The three continuous curves are predicted behavior of oriented oblate spheroids with aspect ratios  $c/a$  equal to 0.995 (bottom curve), 0.25 (middle curve), and 0.01 (top curve), respectively. The corresponding eccentricities are 0.1, 0.968, and 0.999.

ions must go through the carboxylate strata, leading to the observed and predicted sharp rise in CE at low carboxylate concentration. To check this pronounced morphological dependence, the rheology of a 25% carboxylate/75% sulfonate blend is altered to produce the spherical morphology depicted in Figure 3. In contrast to its lamellar counterpart and in agreement with the theoretical pre-



**Figure 3.** Cross-sectional micrograph of a pressed film of similar composition as Figure 1. The rheology, however, has been adjusted to produce abnormal spherical carboxylate domains (arrow). The dark line from upper left-hand corner to central bottom is due to foldover of the microtomed sample film.

**Table I**  
Morphological Dependence of CE for 25%  
Carboxylate/75% Sulfonate Blends of  
Perfluorinated Ionomers

morphology	pred CE	obsd CE
spherical	62%	56%
lamellar	86%	89%

diction, this film has an abnormally low CE as shown in Table I.

In summary, we have extended the effective medium theory to track the morphological dependence of transport and dielectric properties of polymer composites. The utility of the theory is demonstrated with a successful delineation of ion selectivity in physical blends of two incompatible perfluorinated ionomers. Ways to improve and generalize this theory are discussed.

## References and Notes

- (1) Hobbs, S. Y. in "Plastics Polymer Science and Technology"; Baijal, M. D., Ed.; Wiley-Interscience: New York, 1982; pp 274-279.
- (2) Hsu, W. Y.; Giri, M. R.; Ikeda, R. M. *Macromolecules* **1982**, *15*, 1210 and references therein.
- (3) Straley, J. P. *Phys. Rev. B* **1977**, *15*, 5733. Cohen, M. H.; Jortner, J.; Webman, I. *Phys. Rev. B* **1978**, *17*, 4555 and references therein.
- (4) Wood, D. M.; Ashcroft, N. W. *Philos. Mag.* **1977**, *35*, 269. Cohen, M. H.; Jortner, J. *Phys. Rev. Lett.* **1973**, *30*, 696 and references therein.
- (5) Oriented spheroids are assumed to simplify the presentation and mathematics. The full conductivity and depolarization tensors are needed for ellipsoids of random orientations. Spheroids used in this model are either prolate ( $a \geq b = c$ ) or oblate ( $a = b \geq c$ ), where  $a$ ,  $b$ , and  $c$ , are semiprincipal axes of an ellipsoid. The axis of revolution for the spheroid is along the semimajor axis  $a$  for the prolate case and along the semiminor axis  $c$  for the oblate case.
- (6) The eccentricity  $e$  of a spheroid is  $[1 - (c/a)^2]^{1/2}$ , where  $0 \leq c/a \leq 1$  is the aspect ratio. When  $e$  increases from 0 to 1, the spheroid morphology changes continuously from spherical to fibrillar in the prolate case and from spherical to lamellar in the oblate case.
- (7) For transport and dielectric considerations, the appropriate susceptibilities are the conductivity  $\sigma(\omega)$  and dielectric function  $\epsilon(\omega)$ , respectively. Each could be complex, but usually either the real or the imaginary component dominates, except under resonance.
- (8) Stratton, J. A. "Electromagnetic Theory"; McGraw-Hill: New York, 1941; pp 207-217. Note that, for the geometry under consideration, the inside field  $E_i$  is always parallel to the far field (or the mean field)  $E$ .
- (9) See, for example: Funke, K. In "Superionic Conductors"; Mahan, G. D., Roth, W. L., Eds.; Plenum Press: New York, 1976; p 185. The cited relation is in rationalized MKS units; to convert into Gaussian units, replace  $\epsilon_0$  by  $(4\pi)^{-1}$ .
- (10) More exactly, the scaling<sup>11</sup> and analytic<sup>12</sup> theories predict  $\sigma \propto (f - f_0)^t$  above the threshold and  $\epsilon \propto |f - f_0|^{-s}$ , where  $s$  and  $t$  are critical exponents that depend on the effective spatial dimensionality. For a comprehensive discussion of critical exponents, see: Nelson, D. R. *Nature (London)* **1979**, *269*, 379.
- (11) Efros, A. L.; Shklovskii, B. I. *Phys. Status Solidi B* **1976**, *76*, 475.
- (12) Bergman, D. J.; Imry, Y. *Phys. Rev. Lett.* **1977**, *39*, 1222.
- (13) Hori, M.; Yonezawa, F. *J. Math. Phys.* **1975**, *16*, 352. Contributions from pairs, triplets, quadruplets, etc. are systematically added by this scheme.
- (14) Granquist, C. G.; Hunderi, O. *Phys. Rev. B* **1978**, *18*, 1554. This phenomenological method results in replacing the quadratic eq 4 by a higher order algebraic equation; for spherical particles, it is in much better accord with numerical results<sup>3</sup> than simple effective medium theory.<sup>4</sup>
- (15) Davidson, A.; Tinkham, M. *Phys. Rev. B* **1976**, *13*, 3261.
- (16) The general chemical formulas for the perfluorinated ionomers are  $[(CF_2)_nCFOR_4SO_3^-]_x$  and  $[(CF_2)_nCFOR_4CO_2^-]_x$ , respectively. The equivalent weight of the ionomers is about 1100.

William Y. Hsu\*

Central Research and Development Department  
E. I. du Pont de Nemours and Company  
Experimental Station  
Wilmington, Delaware 19898

Timothy D. Gierke

Polymer Products Department  
E. I. du Pont de Nemours and Company  
Washington Works, B21  
Parkersburg, West Virginia 26101

Charles J. Molnar

Finishes and Fabricated Products Department  
E. I. du Pont de Nemours and Company  
Tralee Park Plant  
Wilmington, Delaware 19898

Received August 22, 1983

## Implications of the Failure of the Stokes-Einstein Equation for Measurements with QELSS of Polymer Adsorption by Small Particles

We have reported<sup>1,2</sup> that the Stokes-Einstein equation

$$D = k_B T / 6\pi\eta r \quad (1)$$

can fail noticeably for spherical probe particles in polymer-solvent solutions, even though the probe particles are very dilute. Here,  $D$  is the diffusion coefficient,  $k_B T$  is the thermal energy,  $\eta$  is the solution viscosity, and  $r$  is the apparent hydrodynamic radius. This failure, which is not related to the failure of eq 1 in the case of interacting particles, was not altogether unexpected. Equation 1 is based on a continuum description of the solvent (i.e., solvent molecules much smaller than probe particles), but a probe particle in a polymer solution encounters molecules of its own size.

Measurements of  $D$  have been used to observe the occurrence of polymer binding by spherical particles.<sup>3</sup> Conversely, polymer binding to microscopic probe particles obscures experimental tests on  $D$  in polymer solutions.<sup>4</sup> We here discuss how adsorption isotherms may be obtained in a system in which eq 1 fails.

Quasi-elastic light scattering spectroscopy (QELSS) was used to find the diffusion coefficient of carboxylate-modified polystyrene latex spheres (Polysciences, Inc.) of radii